Characterization of an Optical Time Domain Reflectometer Calibrator

Donald R. Larson, Nicholas G. Paulter, Jr. and Kenneth C. Blaney

Abstract: We report the results of an investigation into the signal characteristics and behavior of an instrument used to calibrate Optical Time Domain Reflectometers (OTDRs). This instrument implements the Telecommunications Industry Association standard TIA/EIA-455-226 "External Source Method." Results of calibrations performed at various U.S. Air Force Precision Measurement Equipment Laboratories have included some anomalous pulse delays and our efforts were focused on identifying the cause and developing corrective procedures for this anomalous behavior. We also describe the measurement method and associated uncertainty analysis used to calibrate optical fiber delay lines employed in the calibration of the OTDR calibrator.

1. Introduction

Optical Time Domain Reflectometers (OTDR) are instruments used to characterize the suitability of an optical fiber network for its intended use and to determine the location of faults in the network such as broken fibers or poor connections. An OTDR emits a pulse of optical radiation at nominally the same wavelength as the one used by the optical fiber based transmission system that is being tested. This pulse is coupled into the fiber under test where it propagates to the end of the fiber. The light guided in the fiber experiences Rayleigh scattering and also reflections from various fiber imperfections, connections, and the end of the fiber. Some of this scattered or reflected light is guided back to the OTDR and is sensed by an internal optical detector. The light that is reflected back to the OTDR is displayed as a function of distance. The distance is derived from the pulse delay, the time interval between when the pulse was emitted and when it is detected (round-trip transmission time), and the wavelength-dependent effective-refractive index of the fiber. This displayed signal typically exhibits a negative slope with increasing time, a result of the increasing loss due to scattering with propagation distance. This slope is proportional to the attenuation coefficient of the fiber. The displayed signal may also exhibit abrupt changes in amplitude due to fiber imperfections, connector losses, a break in the fiber, or Fresnel reflections at the end of the fiber. Like all instruments, OTDRs must be calibrated periodically to ensure that they are working correctly and provide measurement results that are accurate and traceable to a national metrology institute such as NIST. Our investigation examines the distance calibration (i.e., the horizontal scale) but does not incorporate attenuation loss (i.e., the vertical scale). OTDRs are widely used, and more than a dozen companies market them in the United States.

Donald R. Larson
Nicholas G. Paulter, Jr.
Quantum Electrical Metrology Division
National Institute of Standards and Technology[1]
Gaithersburg, MD 20899, USA
Email: larson@nist.gov

Kenneth C. Blaney
U. S. Air Force, AFMETCAL
813 Irving-Wick Drive West
Heath, OH 43056-6116, USA

The Telecommunications Industry Association standard TIA/EIA-455-226 [1] lists three methods of calibrating the distance indication of an OTDR. These methods are known as the "External Source Method," the "Concatenated Fiber Method," and the "Recirculating Delay Line Method."

In the "External Source Method," the delay is simulated using a variable delay generator. This method can simulate a wide range of delays and consequently, distances. In operation, the optical output of the OTDR is converted to an electrical signal that triggers the variable delay generator. The delay generator output is used to drive an optical pulse generator, whose output is coupled into the OTDR and simulates a reflected signal. The selected delay simulates the round trip distance that the output pulse from the OTDR would have traveled in an optical fiber when the pulse is reflected from a fiber discontinuity and returns to the OTDR.

The "Concatenated Fiber Method" uses several fibers with calibrated lengths. These cables are connected together (concatenated) in such a way as to introduce reflections back into the OTDR from the end of each of these calibrated lengths of fiber. The OTDR displays the series of reflections at the calibrated distances.

The "Recirculating Delay Line Method" employs a calibrated length of fiber that is formed into a loop by connecting one end to one input of a two by two splitter or bidirectional coupler and the other end to one output of the splitter or coupler. The OTDR is connected to the other input of the splitter or coupler and a reflector is connected to the remaining output of the splitter or coupler. This splits the optical pulse from the OTDR

[1] Quantum Electrical Metrology Division, Electronics and Electrical Engineering Laboratory, Technology Administration, Department of Commerce. Official contribution of the National Institute of Standards and Technology, not subject to copyright in the U.S.A.

into two parts. Half of the pulse is coupled into the loop of fiber. The other half continues to the reflector and is reflected back to the OTDR. The optical pulse propagating in the loop is split and half continues to the reflector and is also reflected back to the OTDR. This process continues and the multiple reflections generate a comb-like signal on the OTDR. The comb spacing is equal to the sum of the length of the input and output arms of the splitter or coupler and multiples of the calibrated length of fiber in the loop. Since the OTDR is designed to display one half the round-trip time, the displayed comb spacing is one half the actual spacing.

The US Air Force Metrology and Calibration Program (AFMETCAL) currently uses the Fiber Optic Calibrator, Universal System (FOCUS)[2], an implementation of the External Source Method, to calibrate the OTDRs in its inventory. The FOCUS is calibrated using optical fiber spools of approximately 1 km, 2 km, and 4 km lengths with pulse time delays calibrated by NIST. Calibration results performed at various US Air Force Precision Measurement Equipment Laboratories (PMELs) have displayed some anomalous distances or pulse delays. An investigation into the behavior and signal characteristics of the FOCUS was undertaken by NIST to identify the cause and suggest corrective measures for this anomalous behavior.

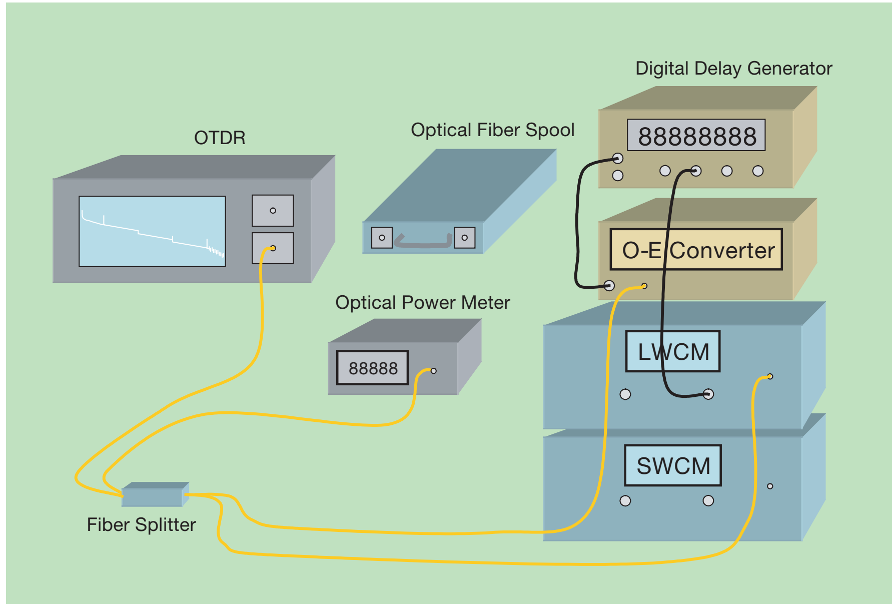

Figure 1. Fiber Optic Calibration Universal System.

2. The FOCUS

The FOCUS consists of three pieces of equipment with an optional fourth instrument that is used if necessary (Fig. 1.) It also includes the optical fiber patch cords and coaxial cables that are required to make the connections necessary for operation. The primary instruments are the Long Wavelength Control Module (LWCM) and Short Wavelength Control Module (SWCM.) The functions of the LWCM and SWCM are to convert the optical pulse emitted by the OTDR to an electrical pulse and to convert an electrical pulse from the digital delay generator (DDG) into an optical pulse that is coupled back to the OTDR. The LWCM and SWCM also contain variable optical attenuators but these are not currently used in the distance or time delay calibrations of OTDRs. The LWCM and SWCM were designed and constructed by Nichols Research Corporation under several Department of Defense contracts. Over 100 of the FOCUS have been produced and sold by Nichols Research worldwide, many to the DOD metrology labs.

The LWCM detects optical pulses in the wavelength range of approximately 900 nm to 1600 nm using an InGaAs photodiode and emits optical pulses at one of two selectable wavelengths, 1310 nm and 1550 nm. The SWCM detects optical pulses in the wavelength range of 600 nm to 1100 nm and emits optical pulses at a wavelength of 850 nm. The third component is the digital delay generator. This is a commercially available, Stanford Research Systems model DG535. This instrument generates, in response to an electrical trigger pulse, an electrical pulse that occurs after a programmable delay. The delay resolution is 5 ps, and the range is 0 to 1000 s. The fourth optional component is an Optical to Electrical Converter (O-E) which was introduced later by Nichols Research. It may be substituted for the optical to electrical converter in the SWCM or LWCM when the optical signal level is too low or when the wavelength is too short for proper operation of the LWCM or SWCM optical receiver. This situation may occur because the optical inputs of the LWCM and SWCM incorporate optical detectors with single mode fiber pigtails. The O-E converter uses a multimode fiber pigtailed optical detector.

In operation, the OTDR optical output pulse is the input to the LWCM, SWCM or O-E converter (Figure 1 depicts input to the O-E). The subsequent electrical output of the LWCM, SWCM or O-E converter then triggers the DDG. After the programmed delay, the electrical pulse output of the DDG is converted by the LWCM or SWCM to an optical pulse that is routed to the OTDR where it is displayed.

3. FOCUS Calibration Procedure

As previously noted, the FOCUS is calibrated using several optical fiber spools of 1, 2, and 4 km lengths with the pulse delays calibrated by NIST. The current FOCUS calibration procedure involves using the NIST-calibrated optical fiber delay lines to generate a reflected pulse

[2] Certain commercial equipment, instruments, or materials are identified in this paper in order to specify the experimental procedure adequately. Such identification is not intended to imply recommendation or endorsement by the National Institute of Standards and Technology, nor is it intended to imply that the materials or equipment identified are necessarily the best available for the purpose.

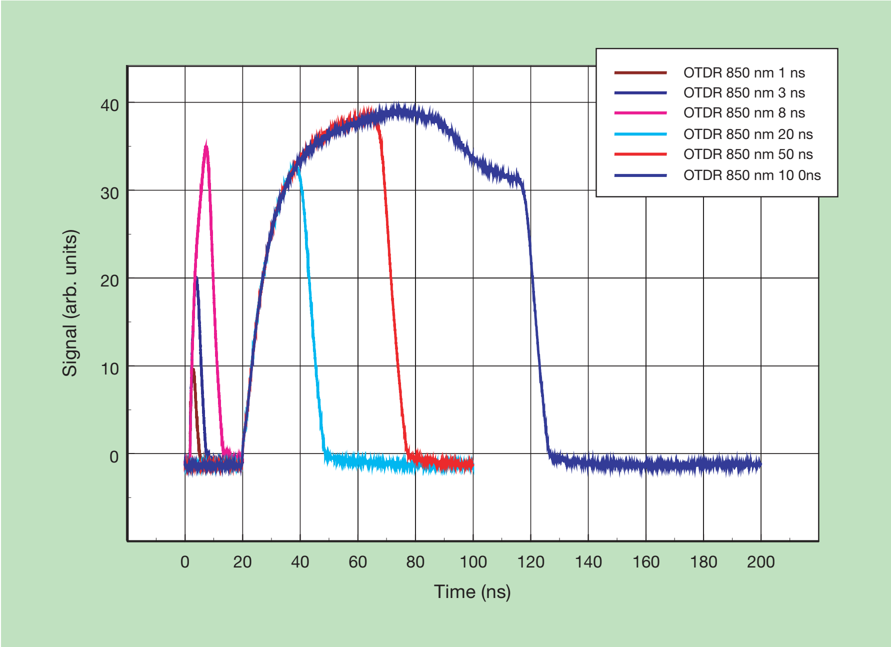

Figure 2. OTDR output at a wavelength of 850 nm showing available pulse widths.

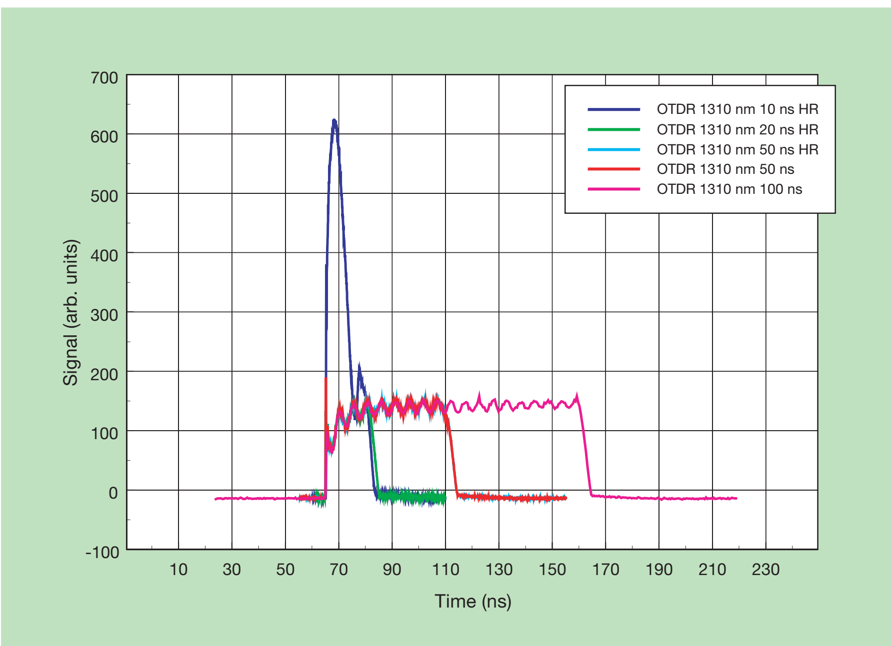

Figure 3. OTDR output at a wavelength of 1310 nm showing available pulse widths (HR = high resolution mode).

signal at a known delay on an OTDR. The FOCUS is then connected to the OTDR and the necessary digitally generated delay is found that produces the same delay as the calibrated optical fiber delay line. The value of the digitally generated delay is compared to the standard, the calibrated delay provided by the optical fiber delay line. The anomalous results were ones that disagreed by more than about 7 ns for a 1 km long optical fiber delay line. A 1 km optical fiber delay line produces a nominal pulse time delay of 5 µs due to the finite transit time. The round-trip time, down the fiber and reflected back up the fiber, measured by the OTDR would be twice that or nominally 10 µs.

After witnessing the calibration of a FOCUS, it was hypothesized that the anomalous results were due to varying levels of optical power being presented to the different optical to electrical converters in the FOCUS or being returned to the OTDR. Since the optical attenuation of an optical fiber delay line increases with length, the use of different length optical fiber delay lines will result in different optical power levels being returned to the OTDR. It was also noted that the biconic optical fiber connectors terminating the optical fiber delay lines exhibited differing amounts of damage or wear. This wear can vary the amount of optical signal attenuation. The optical output signal from the FOCUS, which is intended to simulate the signal returned to the OTDR by the NIST-calibrated optical fiber delay line, is set to a fixed power level of –27 dBm. This power level is not adjusted to simulate the losses due to different length optical fiber delay lines or connector condition. As part of the FOCUS calibration procedure and before any measurements are made, the trigger level of the DDG is set to a predetermined value. Typically, the trigger level is not adjusted to compensate for the varying levels of optical power delivered to the optical to electrical converters in the FOCUS from the OTDR through the optical fiber splitter or patch cords unless the resulting trigger signal amplitude is below the DDG trigger level. The resulting variation in trigger pulse amplitude and pulse shape were thought to produce the variations in measured delay and thus the anomalous results obtained during calibration of the FOCUS. Air Force metrologists had also noted a possible correlation of anomalous results with the duration of the optical pulses selected for output from the OTDR and DDG.

4. Signal Sources and Signal Characteristics

In an attempt to verify this hypothesis, all optical pulses (850 nm, 1310 nm, and 1550 nm wavelengths) generated by the OTDR and FOCUS LWCM and SWCM were examined. The electrical pulses generated by the FOCUS LWCM and the Optical to Electrical Converter (OTDR Calibrator) were also examined as a function of the optical power level used to excite them. The signal sources con-

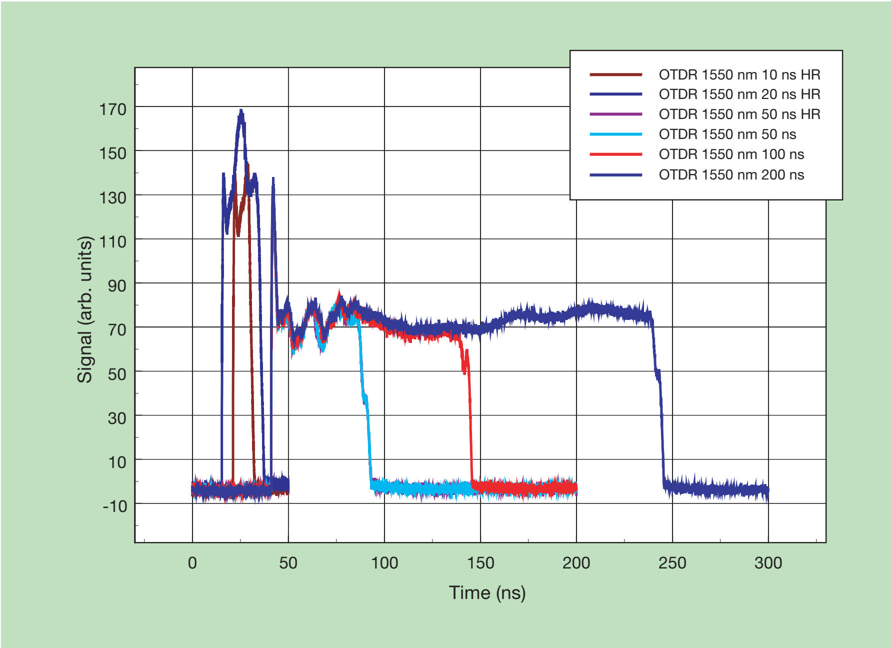

Figure 4. OTDR output at a wavelength of 1550 nm showing available pulse widths (HR = high resolution mode).

sidered here are the optical output of the OTDR, the electrical output of the O to E converter or the electrical output of the LWCM or SWCM, the electrical output of the DDG, and the optical output of the LWCM or SWCM. The signal characteristics considered are the pulse amplitude and monotonicity of the first transition. Since each instrument triggers the next instrument, the amplitude and the monotonicity of the first transition of the output signal will affect the instant at which the next instrument is triggered and the occurrence of the subsequent output.

4.1 OTDR Output Optical Pulse

The OTDRs used were a Tektronix OTDR, model TFP2A provided by the Air Force Metrology and Calibration personnel and a Tektronix OTDR model TFP2 that was purchased by NIST for this project. These OTDRs were capable of generating pulses at three wavelengths, 850 nm, 1310 nm and 1550 nm. The duration and amplitude of the pulses were characterized for all of the various pulse duration settings (Figs. 2 thru 4 respectively).

The pulse durations were found to be approximately equal to the pulse duration setting. The pulse shapes and amplitudes varied significantly with the duration and wavelength selected. For example, the 850 nm wavelength source (Fig. 2) produced pulses that generally increased in amplitude with increasing pulse duration. However, for the 1310 nm wavelength (Fig. 3), the amplitude of the 10 ns pulses were much greater than the amplitudes of the pulses with longer durations. The 1550 nm wavelength source, for pulse durations greater than or equal to 50 ns, produced pulses that exhibited a large post transition overshoot (Fig. 4). A high resolution mode (HR) was available for the 1310 nm and 1550 nm wavelength outputs. The pulse amplitude and duration did not appear to depend on the whether or not the high resolution mode (HR) was used (Figs. 3 and 4).

4.2 Optical Attenuation Dependence Measurements

To simulate the attenuating effects of different lengths of optical fiber (used in the optical fiber delay lines) and varying amounts of connector damage, the optical pulses produced by the OTDR were routed through a programmable variable optical attenuator. The relative amount of attenuation was checked using an optical power meter. The variable optical attenuator was also carefully checked to ensure that the delay it introduced did not vary with the attenuation selection. This was done by connecting the input of the attenuator to a subpicosecond optical pulse source (mode-locked fiber laser) and connecting the output of the attenuator to a fast optical detector (50 GHz bandwidth) and 50 GHz bandwidth sampling oscilloscope. The measurement resolution was approximately 1.0 ps. The output of the fast optical detector was an impulse and the location of the peak on the time axis was not observed to change as the attenuation setting was changed. The insertion loss of the optical attenuator was 3 dB. The spectral range of the variable optical attenuator was 1200 nm to 1650 nm, thus attenuation measurements at a wavelength of 850 nm were not possible under this controlled condition. Some measurements were made at a wavelength of 850 nm using a manually variable optical attenuator. Although the repeatability and control were poor, the results obtained using 850 nm wavelength optical pulses were similar to the results using the 1310 nm and 1550 nm wavelength optical pulses.

4.3 LWCM Output Electrical Pulse

A 10 ns pulse at 1310 nm from an OTDR was used to test the electrical output of the FOCUS LWCM. The electrical output of the LWCM exhibited significant changes in pulse shape as the input optical power level launched into the Optical I-O port was varied (Figure 5). Pulse broadening and significant (50 %) ringing were observed. The slope of the first transition (rising edge) was fairly constant, from 0 dB to 11 dB of attenuation, a change of less than 0.7 ns was observed in the transition occurrence instant. The second transition occurrence instant (falling edge) exhibited significant changes as a function of optical power. The slope of the first transition does show an aberration or shoulder near the high state. If the amplitude changed and this lower slope region moved below the DDG trigger level, an additional delay of several nanoseconds would be introduced.

4.4 SWCM Output Electrical Pulse

As previously noted, the spectral range of the optical attenuator did not cover

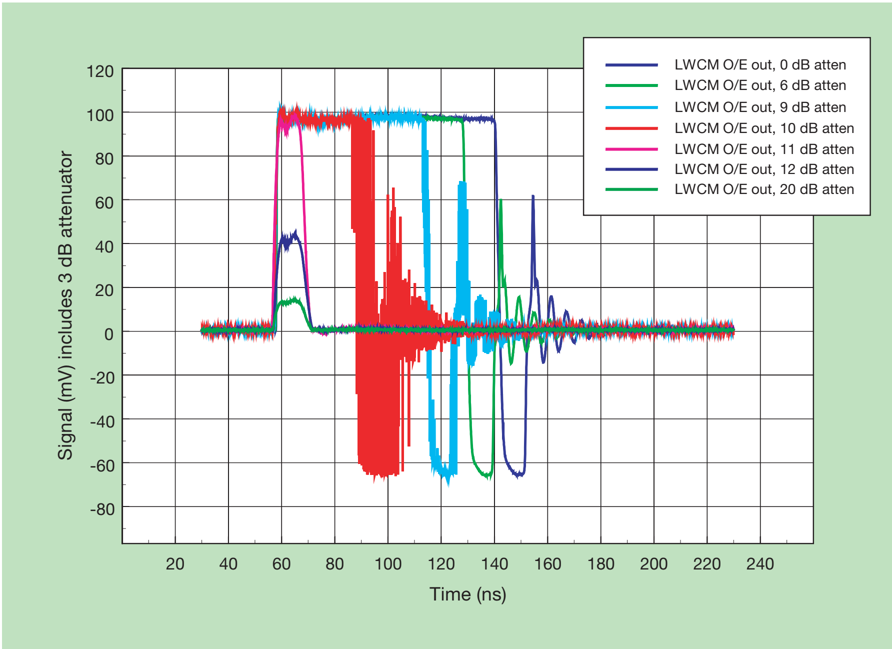

Figure 5. Electrical signal from FOCUS LWCM for various levels of optical attenuation. 10 ns pulse at 1310 nm excitation from OTDR.

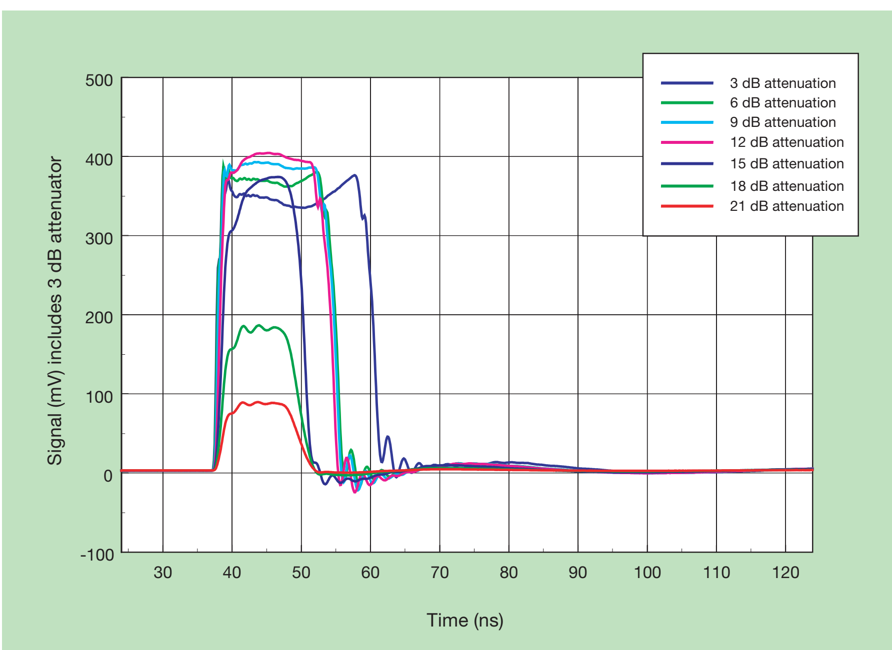

Figure 6. Output of O-E converter at various levels of attenuation for a 10 ns pulse at 1310 nm wavelength excitation from the OTDR.

850 nm, so no measurements with controlled variation of the optical power level were possible. The SWCM electrical to optical converter was later used to generate pulses at a wavelength of 850 nm for calibrating the optical fiber delay lines. Similar behavior to the LWCM was observed.

4.5 O-E Converter Output Electrical Pulse

The shape of the pulse from the electrical output of the Optical to Electrical Converter was more stable than the LWCM as the optical power launched into the optical input port was varied (see Fig. 6). The slope of the first transition (rising edge) was fairly constant from 3 dB to 15 dB of attenuation, a change of less than 0.7 ns was observed in the transition occurrence instant. Closer examination reveals that an aberration or shoulder, on the first transition begins to appear for attenuations greater than or equal to 6 dB. A change in delay of several nanoseconds would be observed if the optical input power level dropped and the electrical output pulse changed so that the level of the shoulder dropped below the DDG trigger threshold.

4.6 LWCM and SWCM Output Optical Pulses

The DDG outputs electrical pulses of consistent amplitude and transition duration. These electrical pulses are a triggered signal and so are consistent even if the trigger is not. These very consistent electrical pulses drive the LWCM and SWCM that generate optical output pulses that are then coupled into the optical fiber from the OTDR. The optical output pulses from the LWCM and SWCM are thus very constant in amplitude and duration. When the output of the OTDR was varied, as suspected, the first transition occurrence instant [2] of the optical pulses output by the LWCM and SWCM did vary as depicted in Fig. 7. Over 3.5 ns of delay change was observed as the attenuation of the OTDR output was changed by only 4 dB. This significant change in delay with optical attenuation is caused by the appearance of the aberration or shoulder on the first transition of the LWCM mentioned in section 4.3 (also exhibited by the SWCM and O-E Converter) near the trigger level of the DDG. In Fig. 7, the rate of change in delay with attenuation is seen to increase for the levels of attenuation used; this is also thought to be a result of the aberration or shoulder in the first transition of the LWCM output electrical pulse.

5. Temperature Effects

Three spools of single mode (at 1310 nm and 1550 nm wavelength) optical fiber, a 4 km NIST-calibrated optical fiber delay line made by Ditel, a 1 km spool of 900 µm diameter tight buffered fiber, and a 1 km coated fiber (250 µm diameter) spool were tested for pulse time

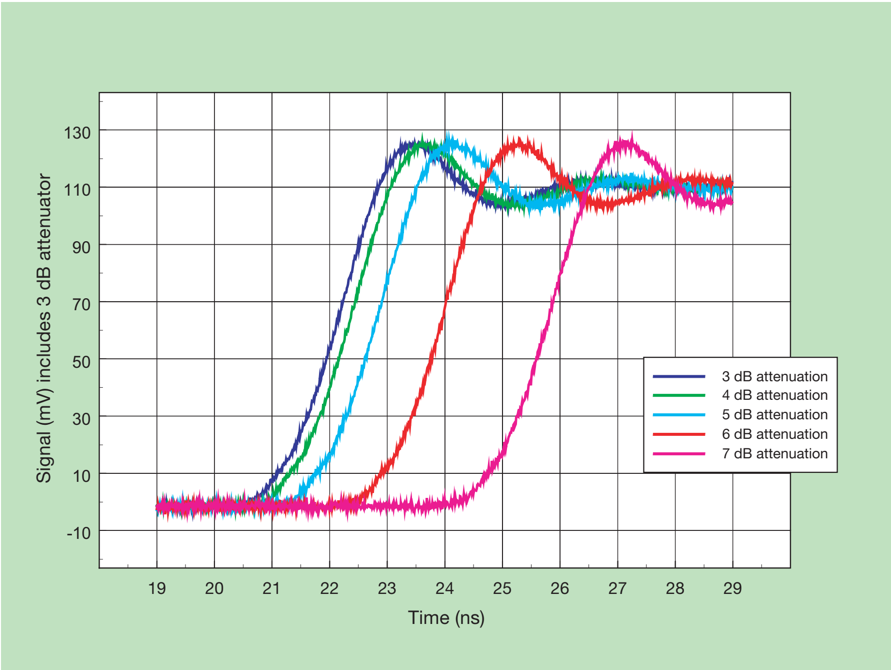

Figure 7. Optical output of LWCM depicting delay variation as OTDR output power is varied.

delay change as a function of temperature. The temperature dependence of pulse time delay of the 900 µm, 1 km long fiber spool was found to 55 ps/(km·°C). The linear coefficient of thermal expansion of fused silica, the temperature dependence of refractive index, and stress induced changes in refractive index are thought to be the causes [3]. Stress may arise from two sources. First, the fiber is 125 µm diameter fused silica but is coated with two kinds of plastic, a pliable coating that brings the diameter to 250 µm and a stiff plastic coating that results in a 900 µm diameter. Plastics have a much larger thermal expansion coefficient than fused silica (550×10^{-9} m/(m·°C)). The 900 µm buffer is polyvinylchloride (PVC) and has a linear thermal expansion coefficient of 70×10^{-6} m/(m·°C). The rubbery coating used to bring bare, 125 µm diameter fiber up to 250 µm diameter is polymethylacrylate, and it has a thermal expansion coefficient of 68×10^{-6} m/(m·°C). Second, the fiber is on a plastic spool, the diameter of which would change with temperature. The temperature dependence of delay for the coated fiber was determined to be 38 ps/(km·°C). The temperature dependence of the 4 km Ditel optical fiber delay line was 33 ps/(km·°C). The Ditel optical fiber delay line appears to be coated fiber that is potted in a metal box. It is not known or discernable if the fiber is wound on a spool inside the metal box. If this 4 km optical fiber delay experiences a temperature change of 7.6 °C, a 1 ns change in delay would be observed. It can be concluded that temperature change is not a significant contributor to the 7 ns anomaly.

6. OTDR Susceptibility to Excess Reflected Power

The manufacturer's resolution specification is 0.1 meter for 1310 nm and 1550 nm wavelengths and 0.01 m for 850 nm wavelength. The resolution of the Tektronix TFP2 OTDR was checked in the expansion mode at approximately 1 km and at 1310 nm wavelength. The minimum change in position indication was 0.1 meter as anticipated. This corresponds to a time resolution of approximately 1.0 ns (round-trip propagation time). The pulse position, taken as the first deviation of backscatter from uniform fiber attenuation, displayed on the OTDR was observed to vary with reflected or returned optical power. The position changed by 1 meter or approximately 10 ns as the optical power from the FOCUS LWCM varied by 10 dB. This change was found to be dependent on the optical pulse duration, 10 µs long pulses yielded the delay reported here and shorter pulses (10 ns, 100 ns and 1 µs) caused a lesser change in delay with optical power but much more variation in the vertical position of the transition. The source of this effect is thought to be related to the saturation of the optical detector and amplifier in the OTDR. The 10 µs duration pulses are thought to cause a deeper saturation. This effect is large enough to significantly contribute to the anomaly.

7. DDG Unexpected Behavior

While attempting to use the DDG as part of the optical fiber delay line calibration, it was observed to exhibit a change in delay that was dependent on the trigger frequency. A deviation of several hundred picoseconds from the set delay resulting from changes in trigger frequency is documented by the manufacturer at the end of the "Guide to Operations" section of the Operation and Service Manual. Three DDG were tested and all displayed this variation in delay with trigger frequency but the amount of delay was different for each. For a delay setting of 20 ms, the variation ranged from 200 ps to over 600 ps as the trigger rate was varied from 25 kHz to 10 MHz. This indicates that the trigger rate of the DDG should be kept constant. Since the trigger rate is determined by the OTDR output, trigger rates may vary with different models or manufacturers OTDRs. This is a small contributor but should be included in any uncertainty analysis when a variety of make and model OTDRs are tested.

8. Biconic Optical Fiber Connectors

The NIST-calibrated optical fiber delay lines used by the Air Force are terminated with biconic optical fiber connectors. The Tektronix TFP2 and TFP2A OTDRs use several other styles of optical fiber connectors and the FOCUS uses FC/PC connectors. This necessitates the use of hybrid optical fiber patch cords, terminated with biconic on one end and the appropriate FC, ST or other style optical fiber connector on the other. These patch cords become part of the FOCUS. The endfaces of all the biconic

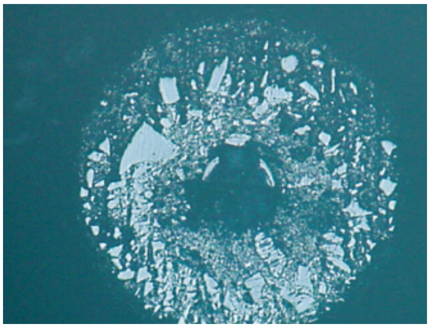

Figure 8. Magnified optical image of the same biconic connector endface after performing the standard cleaning procedure.

connectors on the patch cords (jumper cable) and optical fiber delay lines examined in the course of this work exhibited surface structure which appears to be an epoxy residue or some sort of damage and was not removable using standard cleaning procedures (see Fig. 8, Ditel UTB-1000-184 SM).

The other possibility is that the fiber endface has retracted into the connector and is not actually being contacted by the cleaning paper during the cleaning process. An attempt was made to identify this surface structure which will contribute to varying amounts of insertion loss depending on the proximity of the structure to the fiber core. An optical fiber patch cord with a biconic connector exhibiting this surface structure was subjected to an aggressive cleaning process that included a high-pressure spray of cleaning solvent directed at the fiber endface. This did not change the surface structure. After examination, the same connector was re-polished. This also did not change the surface structure. This indicates that either both surface damage and fiber retraction into the connector are taking place or that neither the high-pressure solvent nor the re-polishing were sufficiently aggressive to remove the surface structure. A hybrid patch cord was ordered to replace the one that was overly polished. This unused biconic connector also exhibited a minor surface structure.

During the FOCUS calibration process, it is necessary to use different patch cords when connecting the optical fiber delay line and then removing it and connecting the FOCUS to the OTDR. An optical fiber splitter is also used to allow measurement of the optical power emitted by the OTDR. This too has biconic and other connectors terminating the fibers. Changing patch cords (jumper cables) during the calibration procedure and from a long lossy fiber spool to an optical pulse source (FOCUS) with interconnecting splitter or patch cords (jumper cables) leads to variations in optical power received by the FOCUS and by the OTDR. The Air Force provided four optical fiber delay lines for this study. On two of the optical fiber delay lines, the insertion loss resulting from the poor condition of the biconic connectors rendered these optical fiber delay lines un-useable. ST and FC fiber connectors are relatively easy to clean and may be re-polished if necessary. The FC is a viable alternative to the biconic.

9. Optical Fiber Delay Line Calibration

The optical fiber delay lines, calibrated by NIST in 1991, were again calibrated for pulse time delay. This was done for two primary reasons. First, replacing the biconic connectors with FC/PC connectors requires cutting off the biconic connectors, they cannot be demounted or removed any other way. A minimum of 3.3 cm of optical fiber is removed when each biconic connector is replaced with an FC/PC connector, this being the length of the biconic connector. Since two connectors must be replaced, a minimum of 6.6 cm of optical fiber is removed. Typically, additional fiber will be lost when terminating the fiber with the new connectors. The minimum uncertainty quoted with the original calibration of these fiber delay lines is ±200 ps for a 1 km length. This uncertainty corresponds to an uncertainty of ±2 cm in the length of the fiber. Therefore, replacing the connectors will result in a delay change greater than the delay uncertainty and necessitates a new calibration of the delay. The other reason to recalibrate the optical fiber delay lines is the unknown stability of the optical fiber with time. The refractive index can change as moisture and hydrogen are absorbed by the fiber. The plastic coatings and buffer layers may also change length and diameter with aging.

The primary function of the optical fiber delay lines is a time delay reference for OTDRs and the FOCUS. These instruments emit optical pulses with unique characteristics and so the OTDR should be calibrated using similar optical pulses. We chose to use the FOCUS as our optical pulse source. It was driven by an electrical pulse generator that was synchronized to a microwave synthesizer. The experimental arrangement is depicted in Fig. 9.

The oscilloscope is used to acquire both the synthesized sinewaves from the microwave synthesizer and the pulses that propagate down the optical fiber delay line. When used to acquire the sinewaves, the oscilloscope is triggered by the pulse from the delay line.

The oscilloscope is also used to "level" these trigger pulses. The optical fiber delay line is somewhat lossy and the pulse amplitude experiences some reduction that is dependent on the length of the fiber delay line being calibrated. When the optical fiber delay line is removed from propagation path, the optical intensity of the optical pulses must be reduced in order to maintain a constant amplitude trigger signal for the oscilloscope. This was accomplished by increasing the selected attenuation in the variable optical attenuator and monitoring the pulse amplitude using the oscilloscope.

The calibration of the optical fiber delay using 850 nm optical pulses is complicated by the fact that the optical fiber used in the Ditel optical fiber delay lines was designed to be single mode at wavelengths of 1310 nm and 1550 nm. At 850 nm, this fiber is multi-mode. Multi-mode fibers, with the 50 µm or 62.5 µm diameter cores allow many optical modes to propagate, and modal dispersion becomes a factor. For these fibers with large diameter cores, launch conditions must be carefully controlled to obtain reproducible results. Since the fiber in these delay lines is single mode at 1310 nm, only a few modes propagate even at 850 nm wavelength. This relaxes the requirements on launch conditions to obtain repeatable results but should still be considered a factor if repeatability problems occur. The full duration at half maximum (FDHM) of the optical pulses propagated in the fiber was approximately 1.2 ns. This duration, with its attendant narrow spectral width, reduced the amount of pulse distortion that is encountered when using shorter pulses typical of very high speed communications links. Modal, chromatic, and polarization mode dispersion are dependent on the spectral width of the launched pulses.

A set of sinewave and trigger pulse data was taken with and without the delay line in the propagation path. The phase of the acquired sinewaves was calculated using a three parameter sine-fitting routine and the average phase change calculated. A coarse measurement of delay was obtained using a 20 kHz sinewave. This frequency was selected because the delay line would introduce a phase shift less than one cycle. The measurement was then refined by measuring the phase shift of a 10 MHz sinewave. The use of a higher frequency sinewave significantly lowered the uncertainty in the measurement results and was possible because the integral number of 2π phase shifts were determined with the initial delay measurement using a lower frequency (20 kHz) sinewave. The acquired sinewaves act as the timing reference for the delay measurement. The frequency of the sinewave is known with much lower uncertainty than the time base of the oscilloscope. The uncertainty in these measurements was determined using the following uncertainty analysis.

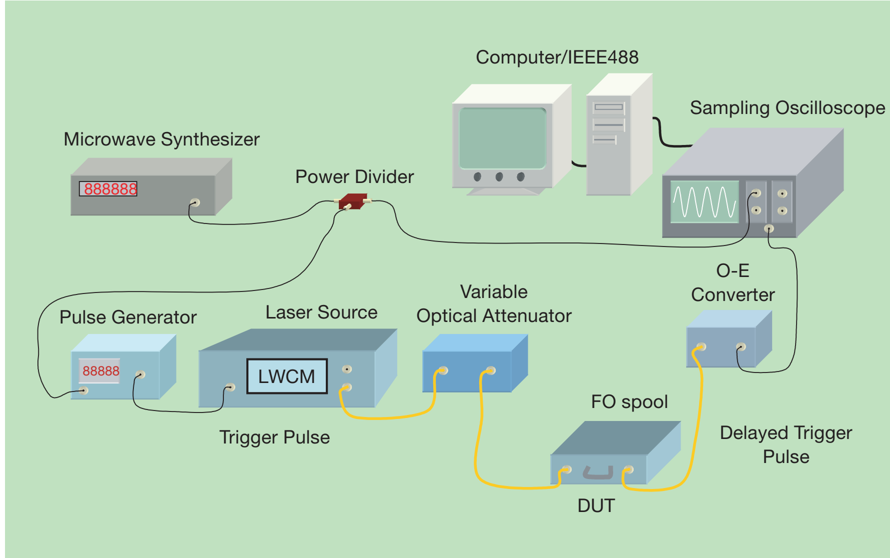

Figure 9. Measurement System For Optical Delay Line Calibration.

10. Uncertainty in Propagation Delay

The delay, D, between two pulses is given by:

$$D = t_{2,R} - t_{1,R} + \Delta D_T \qquad (1)$$

where $t_{1,R}$ and $t_{2,R}$ are the reference level instants for the first pulse (P1) and the second pulse (P2), and ΔD_T is any temperature-induced change in delay. The reference levels are user defined, typically as a fraction (or percentage) of the pulse amplitude. A measurement instrument (oscilloscope, waveform recorder, etc.) is used to acquire the pulse waveforms, P1 (reference pulse) and P2 (delayed pulse), and the reference levels and reference level instants are determined from these acquired pulses using the algorithms defined in the *IEEE Standard on Transitions, Pulses, and Related Waveforms* (IEEE Std 181–2003). [2] The delay may be the result of the introduction of a delay line consisting of a length of coaxial cable or optical fiber.

Another method of determining D uses the measurement instrument to acquire two spectrally pure sets of sinewaves. One set is acquired with the measurement instrument triggered by the undelayed (REF) pulse, P1, and another set is acquired with the delayed (DUT) pulse, P2, providing the trigger. The trigger level for the measurement instrument is set to a fixed level (e.g. 125 mV for a pulse amplitude of 250 mV). If the pulse amplitude is kept constant and if the amplitude of P1 is equal to P2, then the fixed levels may be equivalent to a reference level (e.g. 50 % of pulse amplitude). The trigger instant, t_{tr}, is the instant that the trigger pulse attains the trigger threshold (reference level or fixed level). When these conditions are satisfied, the reference level instants are equivalent to the trigger instant plus a constant, t_0, and may be described by:

$$t_{i,R} = t_{i,tr} + t_0 \, , \qquad (2)$$

where the i subscript may be either 1 or 2. t_0 is either zero or a fixed, measurement-instrument-dependent delay after the trigger instant. Since t_0 is fixed, it may be taken as zero.

Since the acquisition of the sinewaves uses a sampling process, the sinewave may be described by:

$$s[n\delta t] = A \cdot \sin(2\pi f n\delta t + \theta) + V_{offset} \, , \qquad (3)$$

where A is the amplitude of the sinewave, f is the frequency, n is the sample index, δt is the sampling interval, θ is the phase relative to n = 0, and V_{offset} is the voltage offset. The phase, θ, is established by the level of the first sampled element of the sinewave which occurs at $t_{i,R}$ as defined in Eq. 2. From examining Eq. 3, it is apparent that the phase of the acquired sinewave may be described by:

$$\theta_i = 2\pi f t_{i,R} \, . \qquad (4)$$

Solving Eq. 4 for $t_{i,R}$ and replacing the 'i' subscript with a 1 and REF or 2 and DUT subscript to signify the undelayed or delayed trigger instants appropriately yields:

$$t_{1,R} = \frac{\theta_{REF}}{2\pi f} \qquad (5)$$

and

$$t_{2,R} = \frac{\theta_{DUT}}{2\pi f} \, . \qquad (6)$$

Substituting Eqs. 5 and 6 in Eq. 1, the

expression for the delay, D, may now be rewritten as:

$$D = \frac{\theta_{DUT} - \theta_{REF}}{2\pi f} + \Delta D_T \ . \tag{7}$$

The sets of measurements consist of M or N acquired sinewaves, and the delay is found using the difference in the average of the computed phases of the two sets of acquired sinewaves.

$$D = \frac{\frac{1}{M}\sum_{i=1}^{M}\theta_{DUT,\,i} - \frac{1}{N}\sum_{i=1}^{N}\theta_{REF,\,i}}{2\pi f} + \Delta D_T = \tag{8}$$

$$\frac{\bar{\theta}_{DUT} - \bar{\theta}_{REF}}{2\pi f} + \Delta D_T$$

The phase, θ_{REF}, is computed using a sinefitting routine applied to the sinewaves acquired using the non-delayed trigger pulse. Similarly, the phase, θ_{DUT}, is determined by a sinefitting routine applied to the sinewaves acquired with the pulse delayed by the DUT. The last term, ΔD_T, is the effect of temperature on the delay. Although this method uses the phase change of acquired sinewaves to determine the delay, the trigger pulse is the delayed signal. Therefore, this method determines the group delay of the trigger pulse as opposed to the phase delay.

From Equation 8, the uncertainty in the delay D is given by:

$$u_D = \left[\left(\frac{\partial D}{\partial \bar{\theta}_{DUT}}\right)^2 u^2_{\bar{\theta}_{DUT}} + \left(\frac{\partial D}{\partial \bar{\theta}_{REF}}\right)^2 u^2_{\bar{\theta}_{REF}} + \right. \tag{9}$$

$$\left. \left(\frac{\partial D}{\partial f}\right)^2 u_f^2 + \left(\frac{\partial D}{\partial \Delta D_T}\right)^2 u^2_{\Delta D_T}\right]^{\frac{1}{2}} .$$

The partial derivatives (sensitivity coefficients) in (9) are:

$$\frac{\partial D}{\partial \bar{\theta}_{DUT}} = \frac{1}{2\pi f}, \qquad \frac{\partial D}{\partial \bar{\theta}_{REF}} = -\frac{1}{2\pi f}, \tag{10}$$

$$\frac{\partial D}{\partial f} = \frac{\left(\bar{\theta}_{DUT} - \bar{\theta}_{REF}\right)}{2\pi f^2}, \qquad \frac{\partial D}{\partial \Delta D_T} = 1 \ .$$

The various uncertainty components will be considered below.

10.1 Phase Uncertainty

Since separate measurements are used to determine θ_{REF} and θ_{DUT}, each will have a separate uncertainty. However, the measurement method is the same for each and so the uncertainty analysis for one is applicable to both. Equation 4 defines the phase in terms of frequency and the reference level instant. The reference level instant is defined in Eq. 2. Substituting gives the phase in terms of frequency and the trigger instant, t_{tr} and the fixed, measurement-instrument-dependent delay after the trigger instant, t_0:

$$\theta_{REF} = 2\pi f(t_{tr} + t_0), \quad \theta_{DUT} = 2\pi f(t_{tr} + t_0) \ . \tag{11}$$

From Eq. 11, the uncertainty associated with each set of phase measurements is given by:

$$u_{\bar{\theta}_{REF}} = \left[\left(\frac{\partial \theta_{REF}}{\partial f}\right)^2 u_f^2 + \left(\frac{\partial \theta_{REF}}{\partial t_{tr}}\right)^2 u^2_{t_{tr}} + \right. \tag{12}$$

$$\left. \left(\frac{\partial \theta_{REF}}{\partial t_0}\right)^2 u^2_{t_0} + \sigma^2_{\theta_{REF}}\right]^{\frac{1}{2}}$$

and

$$u_{\bar{\theta}_{DUT}} = \left[\left(\frac{\partial \theta_{DUT}}{\partial f}\right)^2 u_f^2 + \left(\frac{\partial \theta_{DUT}}{\partial t_{tr}}\right)^2 u^2_{t_{tr}} \right. \tag{13}$$

$$\left. \left(\frac{\partial \theta_{DUT}}{\partial t_0}\right)^2 u^2_{t_0} + \sigma^2_{\theta_{DUT}}\right]^{\frac{1}{2}}$$

where

$$\frac{\partial \theta_{REF}}{\partial f} = 2\pi\left(t_{tr} + t_0\right), \quad \frac{\partial \theta_{REF}}{\partial t_{tr}} = 2\pi f, \tag{14}$$

$$\frac{\partial \theta_{REF}}{\partial t_0} = 2\pi f \ ,$$

and

$$\frac{\partial \theta_{DUT}}{\partial f} = 2\pi\left(t_{tr} + t_0\right), \quad \frac{\partial \theta_{DUT}}{\partial t_{tr}} = 2\pi f, \tag{15}$$

$$\frac{\partial \theta_{DUT}}{\partial t_0} = 2\pi f \ \cdot$$

The uncertainties in θ_{DUT} and θ_{REF} include the standard deviation, σ_θ, of these phases.

Substituting (14) and (15) into Eqs. 12 and 13 yields:

$$u_{\theta_{REF}} = \tag{16}$$

$$\left[\left(2\pi(t_{1,tr} + t_0)\right)^2 u_f^2 + \left(2\pi f\right)^2 u^2_{t_{1,tr}} + \left(2\pi f\right)^2 u^2_{t_0} + \sigma^2_{\theta_{REF}}\right]^{\frac{1}{2}}$$

and

$$u_{\theta_{DUT}} = \tag{17}$$

$$\left[\left(2\pi(t_{2,tr} + t_0)\right)^2 u_f^2 + \left(2\pi f\right)^2 u^2_{t_{2,tr}} + \left(2\pi f\right)^2 u^2_{t_0} + \sigma^2_{\theta_{DUT}}\right]^{\frac{1}{2}} .$$

It is useful to note that although the trigger process itself is an analog electronic process and not a sampled process, the sinewave from which the phase is determined is acquired by a sampling process. The uncertainty in the trigger instants would normally be one half of the sampling instant but since a fitting routine is used in the sinewave characterization, we have assumed that the uncertainty is approximately:

$$u_{t_{i,tr}} = \pm \frac{1}{20}\delta t . \tag{18}$$

Similarly, even though it is assumed that $t_0 = 0$, t_0 has an uncertainty associated with it. The uncertainty in the trigger instant is also given by:

$$u_{t_0} = \pm \frac{1}{20}\delta t \ . \tag{19}$$

10.2 Frequency Uncertainty

The frequency output by the sinewave generator may be offset from the set frequency and may drift with time and temperature:

$$f = f_{set} + f_{offset} + \Delta f_{time} + \Delta f_{temperature} \ . \tag{20}$$

The manufacturer of the sinewave generator or synthesizer provides a value for the timebase or frequency stability as a function of time and temperature. These parameters may also be determined using proper measurement instruments. According to the manufacturer, the uncertainty in the set frequency, u_{set}, is approximately $10^{-5}f$ and includes any frequency offset. If Δt is the measurement time, σ_T is the standard deviation of the temperature during the measurement process, S_{time} is the timebase stability as a function of time, and $S_{temperature}$ is the timebase stability as a function of temperature, then the frequency uncertainty may be written as:

$$u_f = \left[u_{set}^2 + \left(S_{time}\,\Delta t\right)^2 + \left(S_{temperature}\,\sigma_T\right)^2\right]^{\frac{1}{2}} . \tag{21}$$

The applied sinewave should be free from harmonics and other distortions, and the measuring instrument should not introduce distortions. However, since the settings of the measuring instrument are the same for both sets of sinewave acquisitions, any harmonics and distortions present will be identical for each set and are assumed to cancel when the difference of the phases is calculated.

10.3 Uncertainty Associated with Jitter

Since the acquired signals are sinewaves and signal averaging is used, any jitter present will affect the signal amplitude and not the phase. Therefore, there are no uncertainties associated with jitter.

10.4 Uncertainty Due to Thermal Effects on the Delay

The delay will also be a function of the temperature of the delay line. This is due to temperature dependence of the length and diameter (coefficient of thermal expansion) and the propagation constant (refractive index or dielectric constant) of the fiber. If the change in delay as a function of temperature can be determined for a representative delay line, then the following relation is generalized for delay lines of identical construction.

$$\Delta D_T = \Delta D_L \Delta T L \ . \tag{22}$$

In the above equation, ΔD_L is the change in delay per unit temperature and per unit length, ΔT is the change in temperature, and L is the length of the delay line. The uncertainty due to thermal effects is:

$$u_{\Delta D_T} = \left[\left(\frac{\partial \Delta D_T}{\partial \Delta D_L}\right)^2 u_{\Delta D_L}^2 + \left(\frac{\partial \Delta D_T}{\partial \Delta T}\right)^2 u_{\Delta T}^2 + \left(\frac{\partial \Delta D_T}{\partial L}\right)^2 u_L^2\right]^{\frac{1}{2}} . \tag{23}$$

For the ΔD_L term, what is actually measured is the delay change, ΔD, as a function of temperature and then this quantity is normalized to the length, L_R, of the representative delay line employed. This is described by the equation:

$$\Delta D_L = \frac{\Delta D}{L_R} \ . \tag{24}$$

The uncertainty associated with ΔD_L is:

$$u_{\Delta D_L} = \left[\left(\frac{\partial \Delta D_L}{\partial \Delta D}\right)^2 u_{\Delta D}^2 + \left(\frac{\partial \Delta D_L}{\partial L_R}\right)^2 u_L^2\right]^{\frac{1}{2}} = \left[\left(\frac{1}{L_R}\right)^2 u_{\Delta D}^2 + \left(-\frac{\Delta D}{L_R^2}\right)^2 u_{L_R}^2\right]^{\frac{1}{2}} . \tag{25}$$

The uncertainty in ΔD_L is determined at the time this quantity is measured. Substituting Eq. (25) into Eq. (23) and solving the partial derivatives yields:

$$u_{\Delta D_T} = \left[\left(\Delta T L\right)^2\left[\left(\frac{1}{L}\right)^2 u_{\Delta D}^2 + \left(-\frac{\Delta D}{L^2}\right)^2 u_L^2\right] + \left(\Delta D_L L\right)^2 u_{\Delta T}^2 + \left(\Delta D_L \Delta T\right)^2 u_L^2\right]^{\frac{1}{2}} . \tag{26}$$

The uncertainty in the delay may now be calculated by substituting the above relations into the original Eq. (9):

$$u_D = \left[\left(\frac{1}{2\pi f}\right)^2 u_{\bar{\theta}_{DUT}}^2 + \left(-\frac{1}{2\pi f}\right)^2 u_{\bar{\theta}_{REF}}^2 + \left(-\frac{\bar{\theta}_{DUT} - \bar{\theta}_{REF}}{2\pi f^2}\right)^2 u_f^2 + u_{\Delta D_T}^2\right]^{\frac{1}{2}} . \tag{27}$$

11. The Combined and Expanded Uncertainty

The combined uncertainty is:

$$u_c = u_D = \left[\left(\frac{1}{2\pi f}\right)^2 u_{\bar{\theta}_{DUT}}^2 + \left(-\frac{1}{2\pi f}\right)^2 u_{\bar{\theta}_{REF}}^2 + \left(-\frac{\bar{\theta}_{DUT} - \bar{\theta}_{REF}}{2\pi f^2}\right)^2 u_f^2 + u_{\Delta D_T}^2\right]^{\frac{1}{2}} . \tag{28}$$

The expanded uncertainty is:

$$U_E = k u_c = t_p\left(\nu_{eff}\right) u_c \tag{29}$$

with k, the coverage factor, being found by calculating the degrees of freedom using the Welch-Satterthwaite formula and then setting k equal to the t-distribution for the calculated degrees of freedom to give a 95 % confidence interval.

12. Recommendations

1. Replace biconic connectors with FC/PC connectors.
2. Keep the optical power returned to the OTDR consistent for each calibration of a FOCUS.
3. Record the signal level as well as the position of the OTDR return signal.

4. Set the DDG external trigger level to one half of maximum trigger amplitude. Also set the amplitude to 1.0 V and the offset to 0.0 V.

Some sources of uncertainty were identified for the FOCUS calibration. According to the manufacturer, the accuracy of the delay generated by a DDG is ±1.5 ns (±500 ps typical) plus $1\text{x}10^{-6}$ times the delay setting. An unexpected source of uncertainty was identified in the delay produced by the DDG. The delay was found to vary with trigger rate and the amount of the variation was different for each of three DDG instruments tested. Among the different instruments, the set delay of 20 µs changed by 200 ps to over 600 ps as the trigger rate was varied from 25 kHz to 10 MHz. The delay and pulse amplitude of the DDG should be calibrated.

13. Summary and Conclusions

Two effects are capable of causing the anomalous results in measured time delay, particularly when combined. First, several of the optical and electrical pulse waveforms observed at different points in the signal path do not have monotonically increasing leading transitions, and the transition durations are not short compared to the desired resolution of the time delay estimates. Damaged connectors and different amounts of insertion loss from various optical fiber patch cords and the 2 x 2 coupler cause variations in optical power delivered from the OTDR to the FOCUS. The OTDR optical output pulse amplitude was found to be dependent on selected pulse width. The varying optical power coupled with the non-monotonic transitions cause changes in the Stanford Research Systems model DDG Digital Delay/Pulse Generator trigger instant and thus changes in the time delay. A change in optical power of 4 dB may produce a 3.5 ns change in delay (Figure 7). Second, the delay (length) displayed by Tektronix TFP2 OTDR changes as returned optical power level changes. The distance (delay) changes as much as 1 ns per 1 dB change in signal level. Either of these two effects could account for the anomaly if the power levels changes were great enough. The two effects are not mutually exclusive and may combine to produce the anomalous calibration results observed.

14. References

[1] *Calibration of Optical Time-Domain Reflectometers (OTDR's),* TIA/EIA-455-266, Telecommunications Industry Association, Arlington, VA, May 2002.

[2] *IEEE Standard on Transitions, Pulses, and Related Waveforms,* IEEE Standard 181–2003, The Institute of Electrical and Electronic Engineers, Piscataway, NJ, USA, July 2003.

[3] A.H. Hartog, A.J. Conduit, and D.N. Payne, "Variation of pulse delay with stress and temperature in jacketed and unjacketed optical fibres," *Optical and Quantum Elect.,* vol. 11, pp. 265–273, 1979.